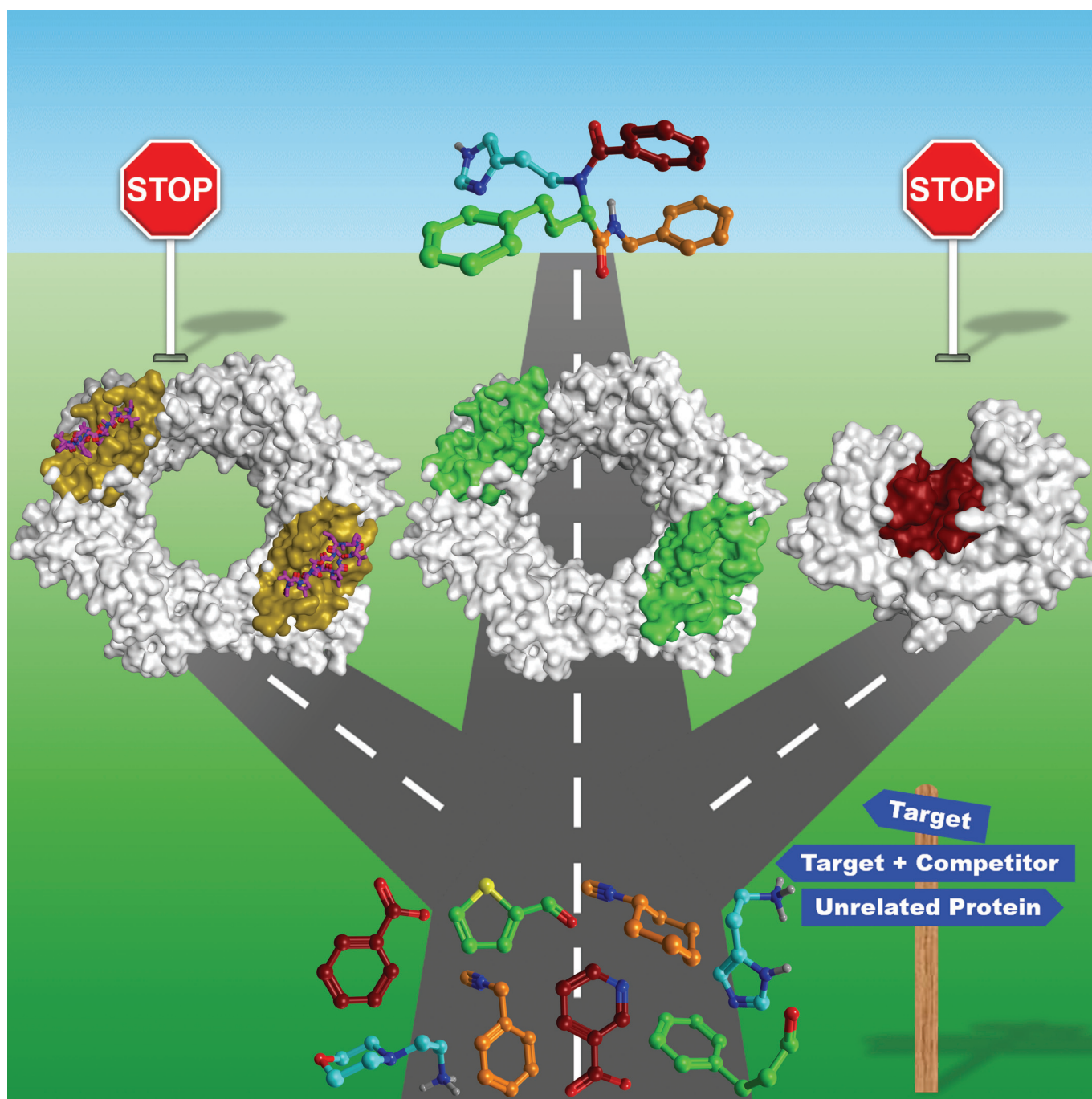


■ Drug Discovery

Protein-Templated Hit Identification through an Ugi
Four-Component Reaction**

Federica Mancini⁺,^[a, b] M. Yagiz Unver⁺,^[a, c] Walid A. M. Elgaher,^[a] Varsha R. Jumde,^[a]
Alaa Alhayek,^[a, b] Peer Lukat,^[d] Jennifer Herrmann,^[e] Martin D. Witte,^[c] Matthias Köck,^[e]
Wulf Blankenfeldt,^[d, f] Rolf Müller,^[b, e] and Anna K. Hirsch*^[a, b, c]



Abstract: Kinetic target-guided synthesis represents an efficient hit-identification strategy, in which the protein assembles its own inhibitors from a pool of complementary building blocks via an irreversible reaction. Herein, we pioneered an in situ Ugi reaction for the identification of novel inhibitors of a model enzyme and binders for an important drug target, namely, the aspartic protease endothiapepsin and the bacterial β -sliding clamp DnaN, respectively. Highly sensitive mass-spectrometry methods enabled monitoring of

the protein-templated reaction of four complementary reaction partners, which occurred in a background-free manner for endothiapepsin or with a clear amplification of two binders in the presence of DnaN. The Ugi products we identified show low micromolar activity on endothiapepsin or moderate affinity for the β -sliding clamp. We succeeded in expanding the portfolio of chemical reactions and biological targets and demonstrated the efficiency and sensitivity of this approach, which can find application on any drug target.

Introduction

The discovery of new bioactive compounds is a long and expensive process, which calls for the development of new techniques that can speed up hit identification and render it more efficient. In this context, target-guided synthesis (TGS) is a powerful approach to discover hit compounds by using the biological target itself in ligand selection. Two main methods, dynamic combinatorial chemistry (DCC) and kinetic target-guided synthesis (KTGS) have emerged.^[1] In KTGS, the target is actively involved in ligand selection by assembling its own inhibitors via an irreversible reaction from a library of complementary building blocks, whereas DCC assembles ligands via reversible processes.^[2–4] Only a few protein-templated reactions

for KTGS have been reported so far.^[5–18] The azide-alkyne cycloaddition was the first reaction used for KTGS^[5,7–9] and is still by far the most widely used. Subsequently, the sulfo-click reaction between sulfonylazides and thioacids,^[10] the amidation between amines and carboxylic acids,^[11,12] the alkylation of thiols by halides,^[13,14] the thio-Michael addition^[15] and the S_N2 opening of epoxides by thiols^[16] were added to the portfolio of protein-templated reactions.^[6,17–19] Stringent requirements need to be met by the irreversible reaction: it needs to be compatible with physiological conditions, the building blocks need to be inert towards biomolecules and a substantial difference in reaction rate between the blank and biomacromolecule-templated reaction is required.

To increase the power and scope of KTGS, it is necessary to expand the number of biocompatible reactions and therefore scaffold diversity. Reactions leading to structural motifs present in numerous protein ligands, irrespective of their target, are particularly desirable. Multicomponent reactions (MCRs) are one-pot reactions, in which more than two starting materials are incorporated to form a new adduct comprising most of the structural motifs of the starting building blocks.^[20] This motivated us and other groups to exploit MCRs for KTGS. The use of Ugi MCRs was first mentioned in a review by Weber but so far no experimental data have been reported.^[18] Only recently, MCRs in protein-templated fragment ligation have re-emerged by the application of a Mannich-3CR for the discovery of STAT5 inhibitors,^[21] in addition to the on-target attempts using the Groebke–Blackburn–Bienaymé 3CR for the discovery of urokinase (uPA) inhibitors.^[22] Herein, we describe the first use of the Ugi-4CR in KTGS for the identification of inhibitors. The Ugi four-component reaction (Ugi-4CR),^[23] is one of the most important MCRs, which affords dipeptide-like structures from isocyanides, carboxylic acids, aldehydes and amines.^[24] Amides are omnipresent in bioactive ligands, which explains why this elegant reaction has found numerous applications in drug discovery, including hit- and lead-identification as well as the generation of large libraries of analogues.^[20,24] Owing to the high exploratory power with regard to chemical space and biocompatibility, it represents an attractive reaction for KTGS.

In the Ugi-4CR-based KTGS, the enzyme templates the synthesis of its own binders from a pool of four types of building blocks. It follows the same concept as other protein-templated reactions in terms of simultaneous binding of building blocks to adjacent pockets of the protein target, enabling the assem-

[a] F. Mancini,⁺ Dr. M. Y. Unver,⁺ Dr. W. A. M. Elgaher, Dr. V. R. Jumde, A. Alhayek, Prof. Dr. A. K. H. Hirsch
 Department for Drug Design and Optimization
 Helmholtz Institute for Pharmaceutical Research Saarland (HIPS)–
 Helmholtz Centre for Infection Research (HZI), Campus Building E8.1
 66123 Saarbrücken (Germany)
 E-mail: anna.hirsch@helmholtz-hips.de

[b] F. Mancini,⁺ A. Alhayek, Prof. Dr. R. Müller, Prof. Dr. A. K. H. Hirsch
 Department of Pharmacy, Saarland University
 Campus Building E8.1, 66123 Saarbrücken (Germany)

[c] Dr. M. Y. Unver,⁺ Dr. M. D. Witte, Prof. Dr. A. K. H. Hirsch
 Stratingh Institute for Chemistry, University of Groningen
 Nijenborgh 7, 9747 AG Groningen (The Netherlands)


[d] Dr. P. Lukat, Prof. Dr. W. Blankenfeldt
 Department of Structure and Function of Proteins
 HZI, 38124 Braunschweig (Germany)


[e] Dr. J. Herrmann, Dr. M. Köck, Prof. Dr. R. Müller
 Department of Microbial Natural Products
 HIPS–HZI, 66123 Saarbrücken (Germany)

[f] Prof. Dr. W. Blankenfeldt
 Institute for Biochemistry, Biotechnology and Bioinformatics
 Technische Universität Braunschweig, Spielmannstr. 7
 38106 Braunschweig (Germany)

[⁺] These authors contributed equally to this work.

[**] A previous version of this manuscript has been deposited on a preprint server (<https://doi.org/10.26434/chemrxiv.11769993.v1>).

 Supporting information and the ORCID identification number(s) for the author(s) of this article can be found under:
<https://doi.org/10.1002/chem.202002250>.

 © 2020 The Authors. Published by Wiley-VCH GmbH. This is an open access article under the terms of Creative Commons Attribution NonCommercial-NoDerivs License, which permits use and distribution in any medium, provided the original work is properly cited, the use is non-commercial and no modifications or adaptations are made.

bly of the corresponding binders. The advantages of the new method over other reported protein-templated reactions are the simultaneous screening of four subpockets and relative ease of accessing structurally complex heterotetrameric binders and their derivatives for further optimization by a one-pot reaction, starting from diverse and synthetically accessible building blocks (Figure 1).

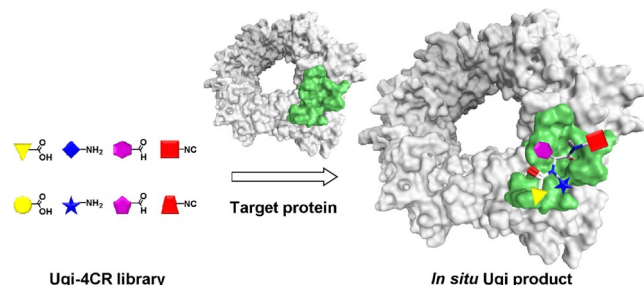


Figure 1. Schematic representation of target-guided Ugi four-component reaction, leading to a dipeptide-like Ugi product from a library of carboxylic acids, amines, aldehydes and isocyanides.

Results and Discussion

In situ Ugi 4-CR using endothiapepsin

To establish a proof-of-concept, we used endothiapepsin as a model target, a member of the class of pepsin-like aspartic proteases, which play a causative role in several diseases such as malaria, HIV, Alzheimer's disease and hypertension. The high degree of similarity to the corresponding drug targets makes endothiapepsin a convenient model enzyme for the elucidation of the mechanism,^[25–27] and the identification of inhibitors of the related drug targets such as renin^[28] and β -secretase.^[29] Moreover, endothiapepsin is a particularly robust enzyme, maintaining its activity for three weeks at room temperature.^[30] Eukaryotic aspartic proteases have two catalytic residues (D35 and D219 in endothiapepsin), which form the catalytic dyad at the core of the active site and cleave the substrate's peptide bond using a bound water molecule.^[25,26]

We designed a novel potential dipeptide-like inhibitor **2** based on compound **1**, which we had reported previously ($IC_{50} = 12.8 \pm 0.4 \mu\text{M}$).^[30] Starting from the X-ray crystal structure of **1** in complex with endothiapepsin (PDB: 4KUP), we used the molecular-modeling software Moloc^[31] and the FlexX docking module in the LeadIT^[32] suite for the structure-based design. Compound **2** features the indolyl moiety as an anchor preserving the most important interactions of **1** in S1 and S2 pockets and in addition benefiting from hydrophobic interactions in S1' and S2' pockets (Figure 2).

To generate the library, we selected two different building blocks for each of the four components (compounds **3–10**, Table 1) with comparable reactivity and solubility. We used benzoic acid as one of the acid components, a negative control for our docking studies as it cannot engage in the same H-bonding interactions with the catalytic dyad as inhibitor **1**. The Ugi-4CR is favored at high concentrations (0.5–2 M) to afford

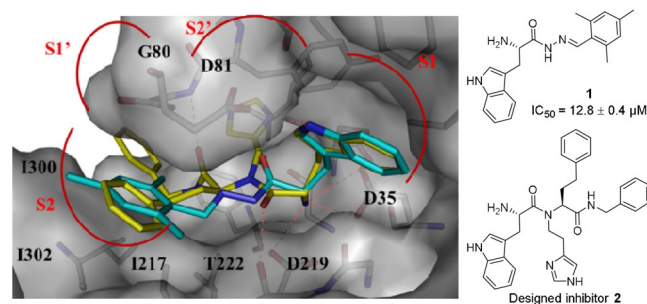
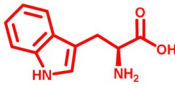
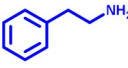
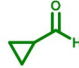

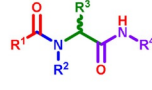
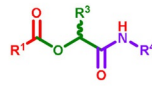
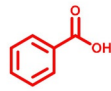
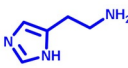
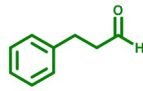
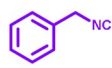
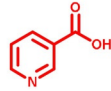
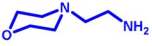
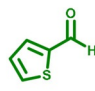

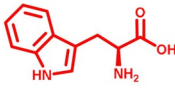
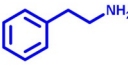
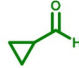



Figure 2. X-ray crystal structure of endothiapepsin in complex with inhibitor **1** (PDB: 4KUP)^[30] superimposed with designed inhibitor **2**. Color code: inhibitor **1** skeleton: C: cyan, N: blue, O: red; inhibitor **2** skeleton: C: yellow, N: blue, O: red; protein backbone: gray; dashed lines: H-bonding interactions below 3.3 Å.

the corresponding products.^[33] The Passerini reaction is the main side reaction of the Ugi-4CR. In this 3-CR, an aldehyde, carboxylic acid and isocyanide react to form α -acyloxyamides.^[34] The mechanism and the products formed are similar for both reactions, which enables the simultaneous screening of a higher number of products than for a single reaction.

Having selected the building blocks, which are commercially available, we set up two reactions in parallel, a protein-templated reaction and a blank reaction, in phosphate buffer (pH 6.8) by mixing the carboxylic acids **3** and **4**, amines **5** and **6**, aldehydes **7** and **8**, and the isocyanides **9** and **10** to reach a final concentration of 100 μM of each component in a total volume of 1 mL phosphate buffer containing DMSO 10% (v/v) (Scheme S1). The optimized reaction conditions have a building-block concentration of 100 μM to minimize product formation in the background reaction and to reduce the amount of protein used. High stability of endothiapepsin allowed us to use up to 10% DMSO to assure complete solubility of the building blocks and the prospective Ugi-4CR products. To the protein-templated reaction, we added a catalytic amount of endothiapepsin (25 μM final concentration) and analyzed both reaction mixtures after 18 h by using UPLC-TQD-SIR (SIR = selective-ion recording) for each of the possible 48 Ugi and 16 Passerini products considering the bifunctionality of L-Trp and diastereomers formation. The SIR technique enables fast and sensitive screening of specific molecular weights (MWs) even at very low concentrations. By screening eight MWs per injection using the same concentrations for protein-templated and reference reactions, we analyzed each reaction in three SIR measurements and detected the formation of two Ugi products **2** and **11** only in the presence of endothiapepsin after 18 h at retention time (t_R) 11.66 and 10.78 min, respectively (Figures S1–S4). To demonstrate that the active site of endothiapepsin is required for product formation, we repeated the reaction in the presence of 25 μM bovine serum albumin (BSA) as an orthogonal protein, and in the presence of a strong competitive inhibitor of endothiapepsin, saquinavir (100 μM , $K_i = 48 \text{ nM}$). No product formation was observed in both control experiments, indicating that binding of the components to the active site of endothiapepsin is essential for their formation (Figures S1 and S3). Worth mentioning, other peaks at different

Table 1. Selected building blocks 3–10 and 21–24 for the in situ Ugi 4-CR using endothiapepsin and β -sliding clamp DnaN.

| Target | Reacting fragments | | | | Ugi-4CR and Passerini-3CR library ^[a] |
|----------------|---|---|---|--|---|
| | R ¹ | R ² | R ³ | R ⁴ | |
| Endothiapepsin |  |  |  |  |  32 possible Ugi products +  16 possible Passerini products |
| |  |  |  |  | |
| |  |  |  |  | |
| |  |  |  |  | |

[a] Each library affords 32 possible Ugi and 16 possible Passerini reaction products for each target including the diastereomeric and enantiomeric pairs.

retention times also appeared in the SIR chromatograms, which do not correspond to the Ugi-4CR products. These peaks could arise from fragmentation of bigger molecules or constitute adducts of smaller fragments.

To check for possible protein modifications in the active site of endothiapepsin, we carried out the following experiments in parallel under identical conditions: the whole library mixture 3–10 incubated with endothiapepsin, the individual building blocks 3, 6–8, and 10 incubated with endothiapepsin, and as a reference only endothiapepsin in the reaction buffer. After 18 h, we evaluated the activity of the enzyme in each reaction using an adaptation of the fluorescence-based assay for HIV protease.^[35] The activity was not affected, demonstrating that no modification had occurred in the active site (Figures S25 and S26).

To investigate whether the individual building blocks bind to endothiapepsin, we used saturation-transfer difference (STD) NMR spectroscopy. STD-NMR enables the characterization of target-ligand interactions in solution. STD-NMR experiments of building blocks 3, 6–8 and 10, which are comprised in the hit compounds' skeleton formed in the protein-templated reaction, showed that all building blocks interact with the target except for aldehyde 7. Lack of interactions between endothiapepsin and 7 may be ascribed to its small size (Figures S6–S10). In addition, we performed competition STD-NMR experiments between each of the above fragments and a known inhibitor of endothiapepsin (bisacylhydrazone 20, IC_{50} = 54 nM).^[36] The results revealed that compound 20 displaces fragments 3 and 6 from the binding site of the enzyme (Figures S12 and S13). Given that 20 is a strong inhibitor and binds in the active site of the enzyme (PDB: 5HCT),^[36] this experiment demonstrates that both 3 and 6 bind to the same pocket of the enzyme as the bisacylhydrazone inhibitor. On the other hand, the signals of fragments 8 and 10 did not dis-

appear in the competition STD-NMR experiment with 20, indicating that they occupy different subpockets of the active site (Figures S14 and S15). As a result, we conclude that the two fragments 3 and 6 bind in the core of the active site of endothiapepsin just like the bisacylhydrazone 20, whereas fragments 8 and 10 occupy alternative, adjacent subpockets, enabling protein-templated formation of the products.

As the in situ Ugi-4CR represents the first example in the field, we synthesized a library of Ugi products to validate its selectivity and to confirm that the formed compounds 2 and 11 are indeed inhibitors of endothiapepsin. The validation library includes all possible eight Ugi-4CR products 2, 11, 13–18 using L-Trp as the acid component and one Ugi-4CR product 19 using benzoic acid (Table 2). Synthesis was accomplished by the reaction of benzoic acid (4) or *N*-Boc-protected L-Trp (12) with the appropriate amine, aldehyde and isocyanide in methanol at ambient temperature, followed by HCl-mediated Boc deprotection of the corresponding Ugi products (Scheme S2). The use of *N*-Boc Trp was necessary to avoid occurrence of the Ugi 5-center-4-component reaction.^[37] We isolated the final compounds as diastereomeric mixtures and used them without further separation.

Biochemical evaluation of the library demonstrated that all combinations with L-Trp as the acid component show activity against endothiapepsin in the IC_{50} range of 1.3–129 μ M. Compounds 2 and 11 are potent inhibitors with IC_{50} values of $1.3 \pm 0.1 \mu$ M and $3.5 \pm 0.1 \mu$ M, respectively (Figures S16 and S18). We could isolate only one diastereomer of inhibitor 2, which showed a slight improvement in activity ($IC_{50} = 0.89 \pm 0.9 \mu$ M) (Figure S17). Further attempts to separate diastereomers of hit compounds 2 and 11 by using various separation techniques failed. Interestingly, compounds 18 and 13 show comparable activity to the hit compounds 2 and 11 (Table 2). This could be due to the content ratio of the synthesized diastereomeric mix-

Table 2. Inhibitory activities of synthesized compounds selected from the KTGS library on endothiapepsin.

| Compound | Structure | IC ₅₀ (μM) | Compound | Structure | IC ₅₀ (μM) |
|----------|-----------|-----------------------|----------|-----------|-------------------------|
| 2 | | 1.3 ± 0.03 | 16 | | 10 ± 5 |
| 11 | | 3.5 ± 0.1 | 17 | | 16 ± 3 |
| 13 | | 6 ± 0.2 | 18 | | 3.3 ± 0.5 |
| 14 | | 129 ± 35 | 19 | | No inhibition at 250 μM |
| 15 | | 19 ± 3 | | | |

tures. The non-observed formation of compounds **18** and **13** by KTGS could be due to a less favorable binding mode and lower affinity of the *tert*-butyl isocyanide compared to the benzyl moiety in **2** and **11**, which are reflected in the inhibitory activities (IC₅₀ values: 3.3 and 6 μM vs. 1.3 and 3.5 μM, respectively). According to our expectation, the analogue **19** with the benzoic acid component did not show any inhibition at the starting concentration of 250 μM (Table 2). These results demonstrate that the *in situ* Ugi-4CR technique is a powerful method, facilitating the selection of the best binders from this library.

In situ Ugi 4-CR using β sliding clamp DnaN

These results motivated us to investigate the scope of the protein-templated Ugi-4CR further. Given that protein–protein interactions (PPIs) are notoriously challenging to inhibit with small molecules, KTGS should represent an invaluable tool to identify a suitable ligand especially when using the Ugi-4CR. Hence, we chose the underexploited antibacterial target DnaN also known as β sliding clamp. This ring-shaped homodimer of two β subunits of DNA polymerase III plays a crucial role during DNA synthesis and repair. Upon formation of a stable clamp around the DNA strand, DnaN interacts with linear motifs of protein binding partners including the DNA polymerases I–V, giving high processivity to DNA synthesis.^[38–40]

Due to its highly conserved structure in bacteria and its structural divergence from its eukaryotic counterpart, proliferating cell nuclear antigen (PCNA), it represents a promising target to develop new antimicrobial agents acting via a novel mechanism. Interactions of DNA polymerases to DnaN occur at a shallow hydrophobic binding site composed of two subsites I and II (Figure 3). Known synthetic DnaN inhibitors hitherto occupy only subsite I and suffer from limited antibacterial activity.^[41–44] On the other hand, the natural antibiotics griselimycins (GMs) are tight binders of the mycobacterial sliding clamp, occupying both subsites I and II.^[45] We expected the powerful combination of KTGS with the Ugi-4CR to address this challenge. Inspection of the X-ray crystal structures of synthetic inhibitors and GMs in complex with DnaN led to the identification of molecular fragments involved in key interactions with DnaN.^[41–45] We utilized these building blocks to generate a virtual library of 320 possible Ugi-4CR and Passerini products including their enantiomers, which we docked into DnaN using MOE software.^[46] Top-ranked ligands such as compound **19** inspired the selection of building blocks for KTGS experiments (Table 1). According to the docking study, compound **19** establishes two hydrophobic interactions with M396 in subsite I and an H-bond between the benzoyl carbonyl and R183. Importantly, the isocyanide component can be accommodated in subsite II (Figure 3).

We ran two reactions in parallel, a protein-templated reaction containing a catalytic amount of *Mycobacterium smegmatis* DnaN (25 μM) and a blank reaction by mixing the building blocks **4**, **6**, **8**, **10** and **21–24** to reach a final concentration of 50 μM of each component in 1 mL phosphate buffer (pH 7, 5% DMSO) and analyzed them by LC-HRMS after 6 h. Notably, due to the high reactivity of the building blocks, lower concentration (50 μM) and shorter reaction time (6 h) were sufficient to detect the change between the protein-templated and blank reactions. Screening for the exact masses of all possible 16 Ugi-4CR (**19**, **25–39**) and eight Passerini products (**40–47**) revealed the amplification of two Ugi products **19** and **25** in the presence of DnaN (Figure 4 and S29–S44). In contrast to the first library used for endothiapepsin, the Ugi derivatives **19** and **25** were also formed in the blank reaction. We observed, however, a marked acceleration of the reaction in the presence

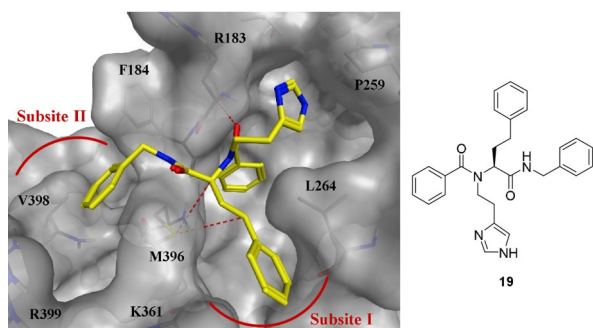


Figure 3. Top-ranked pose of Ugi-4CR derivative **19** (yellow) generated by docking into DnaN (PDB code: 5AGV)^[45] using the scoring function in MOE.^[46] Color code: skeleton: C: yellow, N: blue, O: red; protein backbone and surface: gray; dashed lines: hydrophobic and H-bonding interactions.

of DnaN, leading to an increased amount of the Ugi products compared to the blank reaction (17 to 20-fold for **19** and **25**, respectively) (Figure 4A). We confirmed the identity of the peaks by comparison of the exact masses, fragmentation patterns, and retention times of the compounds formed in situ with those of synthetic references. Furthermore, we quantified the amount of **19** and **25** formed in KTGS and the blank reactions using the synthetic compounds for external calibration (Figure S27 and S28). The peak area of **19** formed by KTGS corresponds to 129 μM (0.004% yield) vs. 5 μM in the blank reaction. The concentration of **25** is equal to 362 μM in the presence of DnaN, in a slightly better yield (0.012%) compared to **19**, vs. 8 μM in the background reaction. These results underline the high sensitivity of HRMS for analyzing KTGS reactions allowing the detection of picomolar quantities of the formed products. To verify that compounds **19** and **25** were selectively templated by DnaN, we repeated the KTGS experiment using endothiapepsin as an unrelated protein. Interestingly, no product formation for **19** and **25** was observed indicating a specific DnaN-templated reaction (Figure 4D). The absence of a background reaction could be due to a non-specific binding of the fragments to endothiapepsin. In agreement with this finding, compound **19** did not emerge in the previous KTGS experiment using endothiapepsin and it showed no inhibitory effect (Table 2). To investigate whether the DnaN-templated reaction occurred in the DNA polymerase binding site or elsewhere, we performed a control experiment in the presence of the tight DnaN binder GM (25 μM) showing no amplification of Ugi products. Thus, binding of the Ugi building blocks indeed takes place in the DNA polymerase interaction site (Figure 4C). To study the reproducibility of hit formation, we repeated the experiments using a new batch of DnaN. The same results were obtained showing significant amplification of compounds **19** and **25** in KTGS (Figure S45), however with lower yields. In KTGS, the concentration of **19** is 22 μM (0.001% yield) vs. 1.5 μM in the blank, while the concentration of **25** is 95 μM (0.003% yield) in KTGS vs. 0.7 μM in the blank. The variation in yields could be attributed to batch-to-batch differences in activity, conformation, and purity of the protein or a change in concentration of building blocks in the DMSO stock solutions.

As observed for endothiapepsin and also by others,^[47] additional peaks were detected in the KTGS experiments even when screening for the exact masses of the Ugi and Passerini derivatives (e.g., Figure 4, Figures S32, S35, and S43). The identity of these peaks was not investigated as they do not match the retention of the synthetic references and do not display any significant amplification.

To evaluate the probability of chemical modification of *M. smegmatis* DnaN by the building blocks, we incubated the protein in the presence and absence of fragments **4**, **6**, **8**, and **10** for 6 h under KTGS conditions. Determination of the molecular mass of DnaN in both samples using ESI-MS revealed no change in the mass demonstrating that no modification occurred (Figure S55).

Since the in situ Ugi-4CR was run at low reactant concentration, we investigated the probability of Ugi-4CR product for-

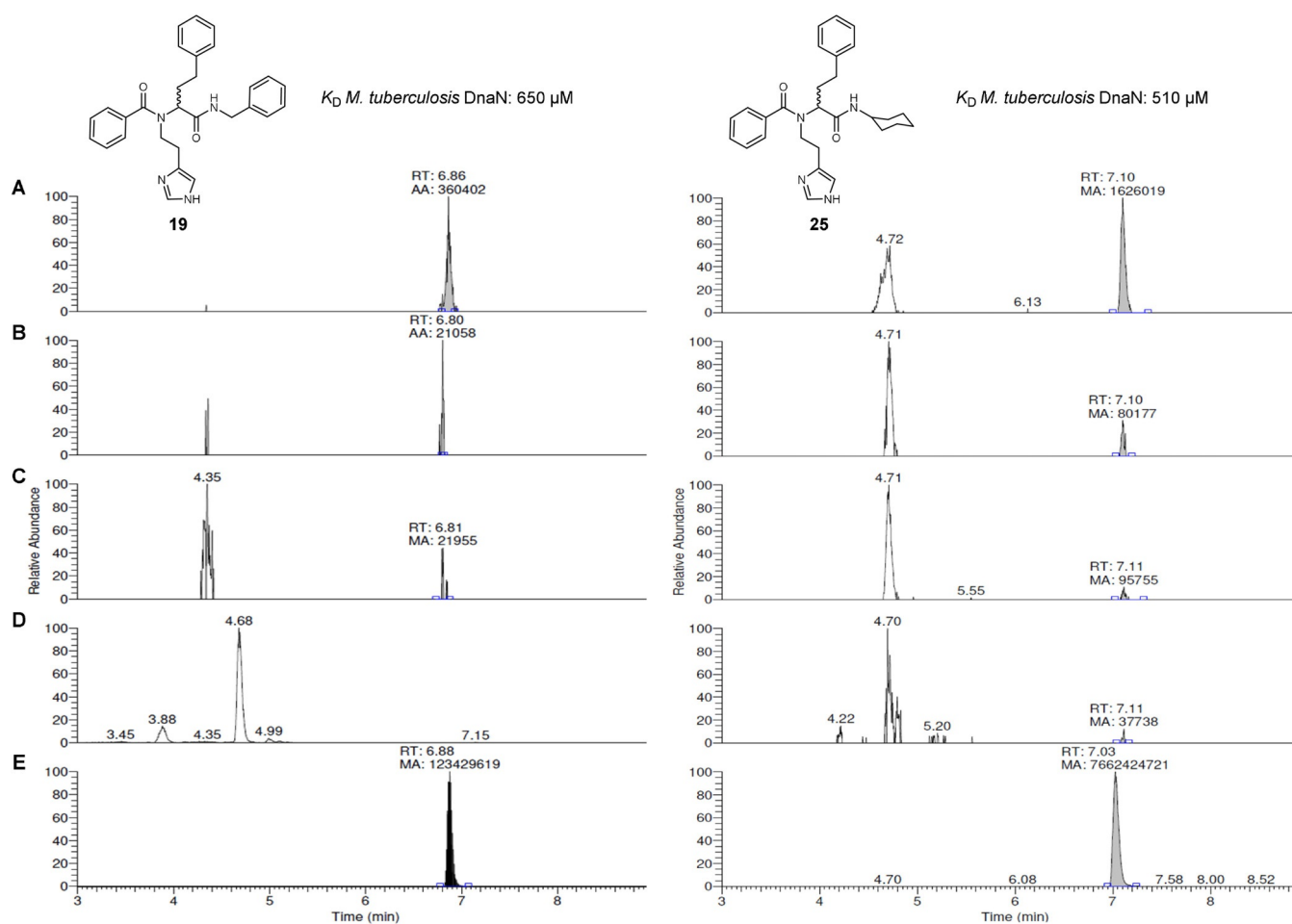


Figure 4. LC-HRMS Hit identification of Ugi-4CR derivatives **19** ($[M+H]^+ = 467.2436$, t_R 6.88 min) and **25** ($[M+H]^+ = 459.2749$, t_R 7.10 min): (A) formation of the hits in the presence of *M. smegmatis* DnaN after 6 h of incubation (B) traces in buffer without protein after 6 h of incubation; (C) suppression of DnaN-templated reaction by GM; (D) templated reaction in the presence of endothiapepsin; (E) reference compounds **19** and **25** obtained by synthetic pathway.

mation with water competing as the acid component.^[48] Monitoring of the eight possible compounds (**48–55**) revealed no or minor formation with no difference between DnaN-templated and blank experiments (Figure S46 and S47).

As some of our fragments bear an activated β -arylethylamine moiety, for example, compounds **3** and **6**, they could undergo Pictet–Spengler cyclization reaction with aldehydes.^[49] Therefore, we monitored the formation of the Pictet–Spengler cyclization products by scanning for their exact masses in DnaN-based KTGS reaction. Interestingly, we detected the formation of a Pictet–Spengler product **56** from histamine **6** and the aldehyde **8** in the DnaN-templated reaction as well as all control experiments, however with only slight amplification in the presence of protein (Figure S48). Although we did not consider compound **56** as a hit, this finding could be very interesting for further investigations of this reaction in KTGS technique.

In order to demonstrate the selectivity of DnaN during the KTGS experiment, we synthesized all possible 16 Ugi products **19**, **25–39** and a representative Passerini compound **40** that contains the same acid, aldehyde and isocyanide components as hit compound **19**. We confirmed the structures of Ugi

compounds **26**, **28** and **35** by X-ray crystallography (Figure S50).

Screening of compounds **19**, **25–40** as racemates for *M. smegmatis* DnaN binding using surface plasmon resonance (SPR) revealed that compounds **19** and **25** display the highest binding responses (Table S9). The equilibrium dissociation constant (K_D) was determined for the hit compounds as well as compound **38**, as a negative control. Compounds **19** and **25** showed low affinity (K_D values: 650 and 510 μM , respectively) for *M. tuberculosis* β -sliding clamp, whereas **38** exhibited much weaker affinity (K_D value: 3200 μM) in line with the KTGS results (Table S10). As a result, we did not proceed to the functional assay, which might be hampered by the solubility limit of the compounds. Nevertheless, we confirmed binding of **19** to *M. tuberculosis* DnaN by STD-NMR revealing that all aromatic protons are in close proximity to DnaN and contribute to binding (Figure S51). This result is in line with the predicted binding mode for compound **19** (Figure 3). Furthermore, we performed a competitive STD-NMR experiment for **19** to verify its binding site using the known inhibitor RU7.^[43] We observed 30–100% reduction of signal intensities for **19** in the presence of RU7 (Figure S53), demonstrating that both compounds bind

to the same binding pocket, in agreement with our KTGS control experiment using GM.

Subsequent evaluation of the antibacterial activity revealed that hits **19** and **25** inhibit the growth of *Escherichia coli* TolC and *Micrococcus luteus* with minimum inhibitory concentration (MIC) values of 128 μM , while none of the compounds shows growth inhibitory effects on *M. smegmatis* (Table S10). Although showing antibacterial effects on Gram-positive and the efflux mutant Gram-negative bacteria, the lack of activity on mycobacteria could hint to a permeability or an efflux issue.

Conclusions

In summary, we described the first in situ ligand assembly using Ugi-4CR, which enables fast screening of a series of compounds that could be expanded to a large number, circumventing the need for synthesis, purification and evaluation of each individual compound. Starting from commercially available building blocks, we screened 64 compounds (48 Ugi and 16 Passerini) by using a catalytic amount of the target protein, demonstrating the efficiency of the in situ Ugi-4CR in KTGS for the discovery of two low-micromolar inhibitors of endothiapepsin. We subsequently applied this powerful strategy to the novel antibacterial target DnaN, resulting in the identification of two binders with decent antibacterial activity. Furthermore, we found that another side reaction, that is, Pictet–Spengler cyclization occurred under the KTGS conditions, which would open a door for studying the utility of this reaction in KTGS. The use of the Ugi-4CR in hit identification holds great potential, in particular for challenging PPI targets such as DnaN and since it enhances the structural diversity of KTGS products. The results obtained through our novel approach will serve as a starting point to develop new Ugi-4CR derivatives with improved affinity and antibacterial activity.

Experimental Section

Crystallographic data

Deposition Numbers 1917479, 1917480, and 1917481 contain the supplementary crystallographic data for this paper. These data are provided free of charge by the joint Cambridge Crystallographic Data Centre and Fachinformationszentrum Karlsruhe Access Structures service.

General protocol for Ugi-4CR-based KTGS using endothiapepsin

Endothiapepsin (25 μL , 1.0 mM in phosphate buffer 0.1 M, pH 6.8) and the 7 building blocks **4–10** (1 μL each, 100 mM stock solution in DMSO), L-tryptophan (**3**) (4 μL , 25 mM stock solution in DMSO) were added to a mixture of DMSO (89 μL) and phosphate buffer (900 μL , 0.1 M, pH 6.8) to give a final concentration of 100 μM of each component in the presence of 25 μM protein. The reaction mixture was allowed to rotate using a rotating mixer at room temperature with 10 rpm. After 18 h, acetonitrile (100 μL) was added to a sample (50 μL) and was centrifuged at 9,727 g for 2 min and the supernatant was collected for analysis. The library was analyzed by UPLC-TQD-SIR [electro-spray ionization (ESI+)] measurement because of its higher sensitivity and greater reliability for product

identification. UPLC-TQD was performed using a Waters Acquity UPLC H-class system coupled to a Waters TQD. All analyses were performed using a reversed-phase UPLC column (ACQUITY HSS T3 Column, 130 \AA , 1.8 μm , 2.1 mm \times 150 mm). Positive-ion mass spectra were acquired using ES ionization, injecting 10 μL of sample; column temperature 35 $^{\circ}\text{C}$; flow rate 0.3 mL min^{-1} . The eluents, water (A) and acetonitrile (B) contained 0.1% of formic acid. The library components were eluted with a gradient from 95% \rightarrow 30% (A) over 20 min, then at 5% (A) over 1 min, followed by 5% (A) for 2 min. The UPLC-TQD-SIR method was used to analyze the formation of Ugi products in in situ and blank reactions. $[M+H]^+$ were monitored using the full mass range to ensure correct isotope patterns for all possible potential Ugi products both for in situ Ugi and blank reactions. The Ugi products in the protein-templated reaction were identified by comparison of their retention time with that of the compound synthesized using conventional methods.

General protocol for Ugi-4CR-based KTGS using DnaN

To investigate the DnaN-templated synthesis, the eight building blocks **4**, **6**, **8**, **10**, and **21–24** (1 μL each, 50 mM stock solution in DMSO) and DnaN (25 μL , 1.0 mM in phosphate buffer 0.05 M, pH 7) were added to a mixture of DMSO (42 μL) and phosphate buffer (925 μL , 0.05 M, pH 7) to reach a total reaction volume of 1 mL containing a final concentration of 50 μM of each component and 25 μM protein. The reaction mixture was allowed to rotate using a rotating mixer at room temperature with 10 rpm. After 6 h, acetonitrile (100 μL) was added to a sample (50 μL), which was centrifuged at 9,727 g for 2 min, and the supernatant was collected for analysis. All analyses were performed using a Thermo Scientific Dionex UltiMate 3000 UHPLC+ focused system with a reversed-phase UPLC column (ACQUITY UPLC BEH C8 Column, 130 \AA , 1.7 μm , 2.1 mm \times 150 mm) coupled to a Thermo Scientific Q Exactive Focus system. Positive-ion mass spectra were acquired using ES ionization, injecting 4 μL of sample; column temperature 35 $^{\circ}\text{C}$; flow rate 0.25 mL min^{-1} . Separations were performed using water (A)/acetonitrile (B) with 0.1% of formic acid. The library components were eluted with a gradient of 90% (A) for 1 min, then from 90% \rightarrow 5% (A) over 9 min, then at 5% (A) over 2 min, followed by 90% (A) for 1.8 min for column equilibration. The identities of the hit compounds **19** (t_R 6.88 of 14.8 min) and **25** (t_R 7.10 of 14.8 min) were confirmed by exact mass and comparison of t_R with the authentic synthesized compounds. For the blank reaction, identical building blocks mixture (1 μL each, 50 mM in DMSO) was incubated in buffer (950 μL , 0.05 M, pH 7) without DnaN and subjected to LC-HRMS analysis. Control experiments using endothiapepsin (25 μL , 1 mM in phosphate buffer 0.05 M, pH 7) instead of DnaN as well as in the presence of the strong inhibitor (25 μL of griselimycin, 1.0 mM in DMSO) were run consecutively as described above. Comparison of the LC/MS chromatograms of these experiments allowed us to determine whether the protein is templating the Ugi-4CR of the building blocks.

Acknowledgements

We would like to acknowledge T. D. Tiemersma-Wegman for help with the UPLC-TOF-SIR measurements, Dr. M. Nuzzolo for help with HPLC measurements, P. van der Meulen for useful suggestions and discussions about STD-NMR spectroscopy, C. Bader for the ESI-MS measurements, Dr. V. Huch for X-ray determinations and Prof. G. Klebe, Prof. A. Dömling, Prof. A. J. Minnaard, Prof. R. W. Hartmann and Dr. M. Mondal for fruitful

discussions. Funding was granted by the German Federal Ministry for Education and Research (grant 16 GW0207K to A.K.H.H., R.M. and W.B.), by the Helmholtz-Association's Initiative and Networking Fund, by the Netherlands Organisation for Scientific Research (NWO-CW, ECHO-STIP grant 717014004), by the Dutch Ministry of Education, Culture, Science (gravitation program 024.001.035) and by the European Research Council (ERC starting grant 757913; all to A.K.H.H.). Open access funding enabled and organized by Projekt DEAL.

Conflict of interest

The authors declare no conflict of interest.

Keywords: drug discovery · kinetic target-guided synthesis · protein–protein interaction inhibitors · protein-templated reactions · Ugi reaction

- [1] M. Jaegle, E. L. Wong, C. Tauber, E. Nawrotzky, C. Arkona, J. Rademann, *Angew. Chem. Int. Ed.* **2017**, *56*, 7358–7378; *Angew. Chem.* **2017**, *129*, 7464–7485.
- [2] E. Oueis, C. Sabot, P.-Y. Renard, *Chem. Commun.* **2015**, *51*, 12158–12169.
- [3] M. Y. Unver, R. M. Gierse, H. Ritchie, A. K. H. Hirsch, *J. Med. Chem.* **2018**, *61*, 9395–9409.
- [4] D. Bosc, V. Camberlein, R. Gealageas, O. Castillo-Aguilera, B. Deprez, R. Deprez-Poulain, *J. Med. Chem.* **2020**, *63*, 3817–3833.
- [5] V. P. Mocharla, B. Colasson, L. V. Lee, S. Röper, K. B. Sharpless, C.-H. Wong, H. C. Kolb, *Angew. Chem. Int. Ed.* **2005**, *44*, 116–120; *Angew. Chem.* **2005**, *117*, 118–122.
- [6] S. E. Greasley, T. H. Marsilje, H. Cai, S. Baker, S. J. Benkovic, D. L. Boger, I. A. Wilson, *Biochemistry* **2001**, *40*, 13538–13547.
- [7] W. G. Lewis, L. G. Green, F. Grynszpan, Z. Radić, P. R. Carlier, P. Taylor, M. G. Finn, K. B. Sharpless, *Angew. Chem. Int. Ed.* **2002**, *41*, 1053–1057; *Angew. Chem.* **2002**, *114*, 1095–1099.
- [8] R. Manetsch, A. Krasniński, Z. Radić, J. Raushel, P. Taylor, K. B. Sharpless, H. C. Kolb, *J. Am. Chem. Soc.* **2004**, *126*, 12809–12818.
- [9] A. Krasniński, Z. Radić, R. Manetsch, J. Raushel, P. Taylor, K. B. Sharpless, H. C. Kolb, *J. Am. Chem. Soc.* **2005**, *127*, 6686–6692.
- [10] X. Hu, J. Sun, H.-G. Wang, R. Manetsch, *J. Am. Chem. Soc.* **2008**, *130*, 13820–13821.
- [11] M. Gelin, G. Poncet-Montange, L. Assairi, L. Morellato, V. Huteau, L. Dugue, O. Dussurget, S. Pochet, G. Labesse, *Structure* **2012**, *20*, 1107–1117.
- [12] M. Jaegle, T. Steinmetzer, J. Rademann, *Angew. Chem. Int. Ed.* **2017**, *56*, 3718–3722; *Angew. Chem.* **2017**, *129*, 3772–3776.
- [13] J. F. Chase, P. K. Tubbs, *Biochem. J.* **1969**, *111*, 225–235.
- [14] R. Nguyen, I. Huc, *Angew. Chem. Int. Ed.* **2001**, *40*, 1774–1776; *Angew. Chem.* **2001**, *113*, 1824–1826.
- [15] E. Oueis, F. Nachon, C. Sabot, P.-Y. Renard, *Chem. Commun.* **2014**, *50*, 2043–2045.
- [16] T. Maki, A. Kawamura, N. Kato, J. Ohkanda, *Mol. Biosyst.* **2013**, *9*, 940–943.
- [17] T. Asaba, T. Suzuki, R. Ueda, H. Tsumoto, H. Nakagawa, N. Miyata, *J. Am. Chem. Soc.* **2009**, *131*, 6989–6996.
- [18] L. Weber, *Drug Discovery Today Technol.* **2004**, *1*, 261–267.
- [19] D. Bosc, J. Jakhlal, B. Deprez, R. Deprez-Poulain, *Future Med. Chem.* **2016**, *8*, 381–404.
- [20] A. Dömling, W. Wang, K. Wang, *Chem. Rev.* **2012**, *112*, 3083–3135.
- [21] E. L. Wong, E. Nawrotzky, C. Arkona, B. G. Kim, S. Beligny, X. Wang, S. Wagner, M. Lisurek, D. Carstanjen, J. Rademann, *Nat. Commun.* **2019**, *10*, 66.
- [22] R. Gladysz, J. Vrijdag, D. van Rompaey, A.-M. Lambeir, K. Augustyns, H. de Winter, P. van der Veken, *Chem. Eur. J.* **2019**, *25*, 12380–12393.
- [23] I. Ugi, C. Steinbrückner, *Angew. Chem.* **1960**, *72*, 267–268.
- [24] P. Slobbe, E. Ruijter, R. V. A. Orru, *Med. Chem. Commun.* **2012**, *3*, 1189–1218.
- [25] L. Coates, P. T. Erskine, S. Mall, R. Gill, S. P. Wood, D. A. A. Myles, J. B. Cooper, *Eur. Biophys. J.* **2006**, *35*, 559–566.
- [26] L. Coates, H. H. Tuan, S. Tomanicek, A. Kovalevsky, M. Mustyakimov, P. Erskine, J. Cooper, *J. Am. Chem. Soc.* **2008**, *130*, 7235–7237.
- [27] L. Coates, P. T. Erskine, S. P. Wood, D. A. A. Myles, J. B. Cooper, *Biochemistry* **2001**, *40*, 13149–13157.
- [28] J. Cooper, W. Quail, C. Frazao, S. I. Foundling, T. L. Blundell, C. Humblet, E. A. Lunney, W. T. Lowther, B. M. Dunn, *Biochemistry* **1992**, *31*, 8142–8150.
- [29] S. Geschwindner, L. L. Olsson, J. S. Albert, J. Deinum, P. D. Edwards, T. De Beer, R. H. A. Folmer, *J. Med. Chem.* **2007**, *50*, 5903–5911.
- [30] M. Mondal, N. Radeva, H. Köster, A. Park, C. Potamitis, M. Zervou, G. Klebe, A. K. H. Hirsch, *Angew. Chem. Int. Ed.* **2014**, *53*, 3259–3263; *Angew. Chem.* **2014**, *126*, 3324–3328.
- [31] P. R. Gerber, K. Müller, *J. Comp. Aid. Mol. Des.* **1995**, *9*, 251–268.
- [32] BioSolveIT GmbH, Sankt Augustin. <http://www.biosolveit.de/LeadIT/>.
- [33] A. Dömling, I. Ugi, *Angew. Chem. Int. Ed.* **2000**, *39*, 3168–3210; *Angew. Chem.* **2000**, *112*, 3300–3344.
- [34] M. Passerini, *Gazz. Chim. Ital.* **1921**, *51*, 126–129.
- [35] M. V. Toth, G. R. Marshall, *Int. J. Pept. Protein Res.* **2009**, *36*, 544–550.
- [36] M. Mondal, N. Radeva, H. Fanlo-Virgý, S. Otto, G. Klebe, A. K. H. Hirsch, *Angew. Chem. Int. Ed.* **2016**, *55*, 9422–9426; *Angew. Chem.* **2016**, *128*, 9569–9574.
- [37] A. Demharter, W. Hörl, E. Herdtweck, I. Ugi, *Angew. Chem. Int. Ed. Engl.* **1996**, *35*, 173–175; *Angew. Chem.* **1996**, *108*, 185–187.
- [38] Z. Yin, M. J. Kelso, J. L. Beck, A. J. Oakley, *J. Med. Chem.* **2013**, *56*, 8665–8673.
- [39] Z. Yin, L. R. Whittell, Y. Wang, S. Jergic, M. Liu, E. J. Harry, N. E. Dixon, J. L. Beck, M. J. Kelso, A. J. Oakley, *J. Med. Chem.* **2014**, *57*, 2799–2806.
- [40] Z. Yin, L. R. Whittell, Y. Wang, S. Jergic, C. Ma, P. J. Lewis, N. E. Dixon, J. L. Beck, M. J. Kelso, A. J. Oakley, *J. Med. Chem.* **2015**, *58*, 4693–4702.
- [41] Z. Yin, Y. Wang, L. R. Whittell, S. Jergic, M. Liu, E. Harry, N. E. Dixon, M. J. Kelso, J. L. Beck, A. J. Oakley, *Chem. Biol.* **2014**, *21*, 481–487.
- [42] G. Wijffels, W. M. Johnson, A. J. Oakley, K. Turner, V. C. Epa, S. J. Briscoe, M. Polley, A. J. Liepa, A. Hofmann, J. Buchardt, C. Christensen, P. Prosselkov, B. P. Dalrymple, P. F. Alewood, P. A. Jennings, N. E. Dixon, D. A. Winkler, *J. Med. Chem.* **2011**, *54*, 4831–4838.
- [43] R. E. Georgescu, O. Yurieva, S.-S. Kim, J. Kuriyan, X.-P. Kong, M. O'Donnell, *Proc. Natl. Acad. Sci. USA* **2008**, *105*, 11116–11121.
- [44] G. Wijffels, B. P. Dalrymple, P. Prosselkov, K. Kongsuwan, V. C. Epa, P. E. Lilley, S. Jergic, J. Buchardt, S. E. Brown, P. F. Alewood, P. A. Jennings, N. E. Dixon, *Biochemistry* **2004**, *43*, 5661–5671.
- [45] A. Kling, P. Lukat, D. V. Almeida, A. Bauer, E. Fontaine, S. Sordello, N. Ziburanny, J. Herrmann, S. C. Wenzel, C. König, N. C. Ammerman, M. Belén Barrio, K. Borchers, F. Bordon-Pallier, M. Brönstrup, G. Courtemanche, M. Gerlitz, M. Geslin, P. Hammann, D. W. Heinz, *Science* **2015**, *348*, 1106–1112.
- [46] Molecular Operating Environment (MOE), 2018.01; Chemical Computing Group ULC, 1010 Sherbooke St. West, Suite 910, Montreal, QC, Canada, H3A 2R7, **2019**.
- [47] M. Whiting, J. Muldoon, Y.-C. Lin, S. M. Silverman, W. Lindstrom, A. J. Olson, H. C. Kolb, M. G. Finn, *Angew. Chem. Int. Ed.* **2006**, *45*, 1435–1439; *Angew. Chem.* **2006**, *118*, 1463–1467.
- [48] L. Weber, S. Wallbaum, C. Broger, K. Gubernator, *Angew. Chem. Int. Ed. Engl.* **1995**, *34*, 2280–2282; *Angew. Chem.* **1995**, *107*, 2452–2454.
- [49] E. D. Cox, J. M. Cook, *Chem. Rev.* **1995**, *95*, 1797–1842.

Manuscript received: May 6, 2020

Accepted manuscript online: May 19, 2020

Version of record online: September 30, 2020